Fibers and Polymers 2005, Vol.6, No.2, 108-112

Properties of Polyacrylonitrile/Single Wall Carbon Nanotube Composite Films Prepared in Nitric Acid

Seong Hoon Kim, Byung Gil Min, and Sang Cheol Lee*

School of Advanced Materials and System Engineering, Kumoh National Institute of Technology, Gumi 730-701, Korea

(Received March 15, 2005; Revised May 14, 2005; Accepted May 21, 2005)

Abstract: Nanocomposite films were prepared by casting the solution of polyacrylonitrile (PAN) and single wall nanotube (SWNT) in nitric acid subsequent to sonication. Even though SWNT shows good dispersion visually, the reinforcing effect was not satisfactory. The G-band Raman spectra of the drawn film clearly demonstrated that SWNTs in the film are well-oriented along the drawing axis of the film. The electrical resistivity of the film prepared using nitric acid was lower than that of the film using DMF. Thus, nitric acid is presumably more effective in dispersing nanotubes than DMF.

Keywords: SWNT, Polyacrylonitrile, Nanocomposite, Nitric acid, Raman spectroscopy

Introduction

In the field of nanotechnology which is believed to have great potential to become a key technology, carbon nanotubes (CNT), due to their unique structure and properties, appear to offer quite promising potential for industrial application [1]. As prices decrease, they also become increasingly affordable for use in structural materials such as polymer composites, and therefore in many large-scale applications such as antistatic or conductive materials [1-3], mechanically reinforced materials [4-6] and flame retarded materials [7-10] today.

Particularly, single-walled carbon nanotubes (SWNT) as fillers in polymer matrix attracted considerable interest due to their unique carbon structure and extraordinary mechanical, thermal, and electrical properties. Due to the difficulties in dispersing CNT in polymer matrix and high cost, most of nanocomposite studies with SWNT have been performed in solution system more than melt system. For the solution system, the selection of chemical solvent is such an important factor that the evaluations on the properties of SWNT/polymer nanocomposites [11]. However, it has been difficult to explore the full potential of these materials due to their insolubility at reasonable concentrations in common solvents. Attempts have been reported to dissolve and characterize SWNT in various organic solvents such as dimethyl formamide (DMF) [12,13].

In recent studies of polyacrylonitrile (PAN)/SWNT composite fibers and films [14,15], prepared in organic solvents such as dimethyl acetamide (DMAc) or DMF, exhibited enhanced mechanical and electrical properties. In this study, we prepared characterized PAN/SWNT nanocomposite films prepared from the solution in nitric acid which is also a good solvent for the commercial production of PAN fibers.

*Corresponding author: leesc@kumoh.ac.kr

Experimental

Preparation of SWNT/PAN Solution and Composite Films

As-prepared (HiPCO 86) SWNT was used without further purification. PAN was supplied by Taekwang Ind. as a copolymer of acrylonitrile and methyl acrylate (M.W. ~ 100, 000 and AN: MA ~ 90:10). Dried SWNT was mixed with 70% nitric acid followed by sonication for 10 hours using a bath sonicator. During the sonication process the mixtures were stirred every two hours interval with a mechanical stirrer for 30 minutes. To this dispersion PAN was added and stirred well and dissolved to get solutions containing PAN and SWNT in the ratios 99:1 and 95:5 as shown in Table 1. Films were prepared by casting the solutions on glass followed by vacuum drying at 50 °C. The as-cast film was drawn on a hot plate up to 5 times of its original length.

Characterization

The morphology and microstructure of the SWNT were characterized using atomic force microscope (AFM) and scanning electron microscopy (SEM). AFM and SEM images were obtained by using a Autoprobe in 5 (Thermo Microscope) and a field emission scanning electron microscope (FE-SEM) of Hitachi (S-4300), respectively. Tensile properties of the films were measured using a universal testing machine (Instron 4467) at a crosshead speed of 100 % per min. The polarized Raman spectra were excited with a Ar^+ ion laser (514.5 nm) and recorded using a Raman spectroscope (SpectraPro-750

Table 1. Composition of SWNT and PAN in nitric acid

Component	Concentration	
	1 wt%	5 wt%
Nitric acid	22.5 g	18 g
SWNT	25 mg	100 mg
PAN	2.5 g	1.9 g

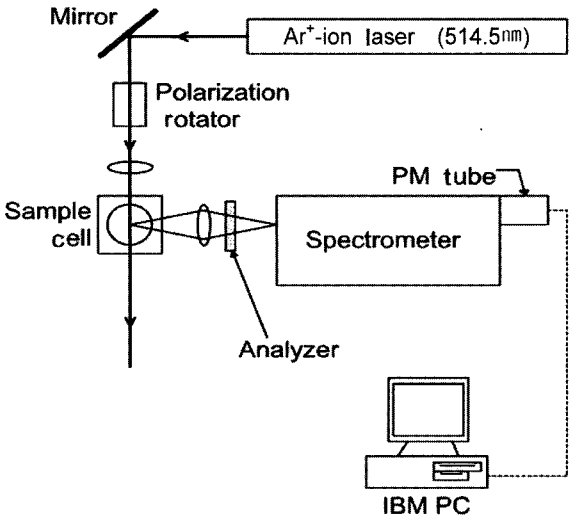

Figure 1. Setup for the polarized Raman spectroscopy.

of Action Research Co.). For the orientation-dependent and polarized measurements a polarizing rotator and an analyzer were set before and after a specimen on a rotating stage, respectively, at the cross-Nicol state (Figure 1). All Raman spectra were taken in backscattering configuration, with the incident and scattered light propagating perpendicular to the specimen film. Electrical resistivity of the neat PAN and PAN/SWNT composite films were measured using Kiethley 2410 sourcemeter at 10 V and 105 mA compliance.

Results and Discussion

Morphology and Mechanical Properties of the SWNT/PAN Composite Films

Figure 2 shows the dispersed state of SWNT in PAN solution in nitric acid. The solution of the SWNT in acetic acid was stable for days. In the optical image, it could be observed that almost all the aggregated nanotubes got dispersed very well except some hard chunks, which might not have been swelled by the sonication process, which has been well demonstrated that sonication of nanotubes in the presence of a solvent is a very good tool for separating the nanotube bundles and dispersing them in the solvent [16-18].

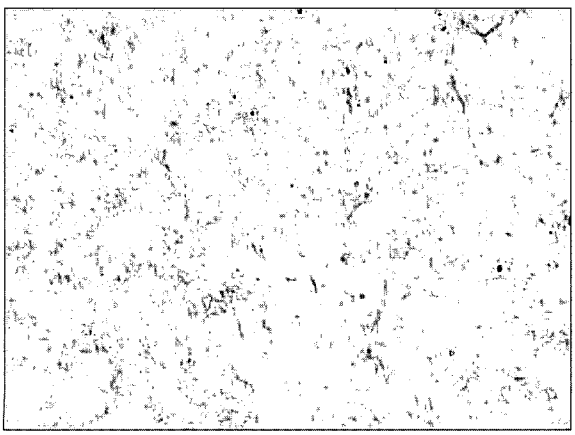

Figure 2. Optical micrographs of solution of PAN/SWNT (99/1 w/w) at 10 wt% in nitric acid.

Figure 3 exhibited the SEM images of the SWNT used in the study and the crack of the composite film. It is seen that the SWNT bundles in bulk state (a) did not exfoliated to the thinner bundle or individual nanotubes after treated by sonication. The crack image (b) shows some broken nanotubes and well rooted in the matrix, which implies that the adhesion between PAN matrix and nanotube bundles.

The typical AFM surface image of SWNT/PAN (95/5) composite film also clearly displays that the SWNTs are dispersed in the film as individual rope or thin bundles of it, as depicted in Figure 4. It is similar to the film prepared from DMF solution [13] Particularly, the AFM image shows that the nanotubes form an interwoven fibrous structure on the surface of the composite film.

Conclusively, the SWNTs could be well dispersed in the polymer matrix when the composite is prepared from solution in acetic acid with help of sonication, even though the ropes

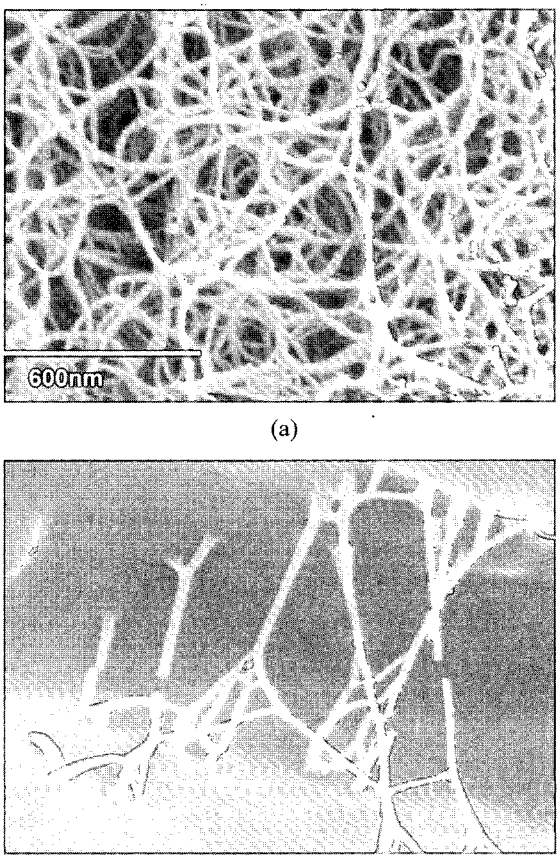

Figure 3. SEM images of unpurified SWNT (a) and the fractured PAN/SWNT (99/1 w/w) composite film (b).

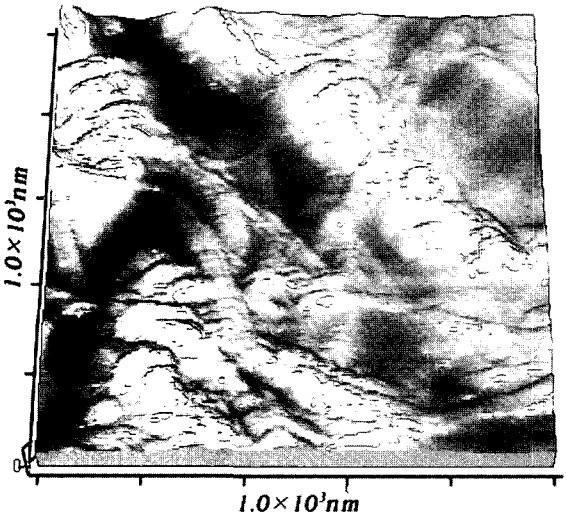

Figure 4. Atomic force microscopic (AFM) surface image of a SWNT/PAN (95/5) composite film showing an interwoven SWNT ropes wrapped by PAN matrix.

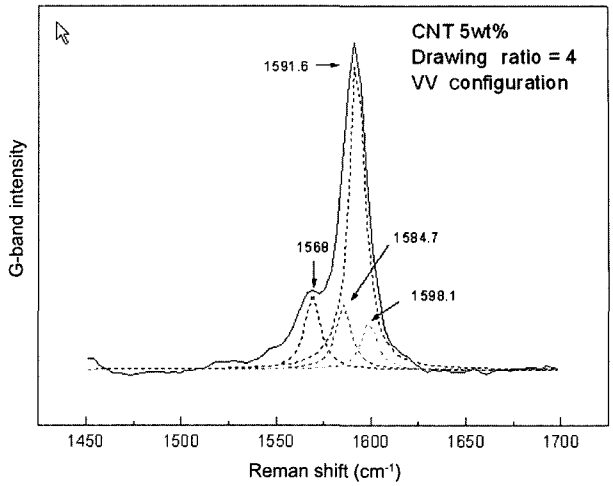

Figure 5. Raman spectrum of PAN/SWNT drawn film with the polarization of the incident laser beam parallel to the drawing axis of the composite film (VV configuration).

Table 2. Tensile properties of the PAN/SWNT drawn films

SWNT content (wt%)	Tensile strength (GPa)	Elongation (%)	Initial modulus (GPa)
0	0.23 ± 0.05	35 ± 5	2.0 ± 0.3
1	0.27 ± 0.05	22 ± 5	2.9 ± 0.5
5	0.15 ± 0.03	10 ± 3	5.0 ± 0.5

are not separated to the individual tubes.

The tensile properties of the drawn composite films are shown in Table 2. The mechanical properties of the composite films were not satisfactoty, which is presumed due to not enough degree of dispersity of SWNT in PAN matrix.

SWNT Orientation in the Drawn Composite Film

Since SWNTs show resonance-enhanced Raman scattering effect when a visible or near infrared laser is used as the excitation source [19-21] and PAN as well as most other polymers do not show such a resonance effect, the Raman spectroscopy is an ideal characterization technique for the orientation study of SWNT [14,15,22].

For the Raman spectra, a fixed polarizer was used to analyzer the scattered light polarized parallel (VV configuration) and perpendicular (VH configuration) to the incident-light polarization. Figure 5 shows a typical VV G-band Raman spectra for the drawn PAN/SWNT(95/5) film. As seen in the figure, the G-line of the graphite at 1580 cm^{-1} is split into several modes when a grapheme sheet is bent to a cylinder, that is, tube shape [23].

Generally for a individual SWNT, VV mode shows maximum intensity when the polarization of the incident radiation is parallel to the nanotube axis ($\theta = 0$ °), while near 90 ° no signal could be detected. On the contrary, VH mode shows maximum intensity when the polarization of the incident radiation is perpendicular to the nanotube axis ($\theta = 45$ °) [23]. Figure 6 displays Raman spectra with different angles (θ) between the polarization (electric field) of the incident laser light and the drawing direction of the film. From the Figure 6(a) and (b) showing, respectively, the VV and VH G-band spectra of the drawn film, it is clearly known that G-band intensity in both modes are dependent on the film rotation, and the intensity of the VV mode is much higher than that of the VH mode. These results mean that SWNTs in the film are well-oriented along to the drawing axis of the film. Moreover, VV mode shows a maximum at ($\theta = 0$ °) and almost no intensity at 90 °, while the maximum of the VH mode at θ = 45 °, as depicted in Figure 6(c) and (d), respectively.

Conclusively, it is considered that high degree of orientation of SWNTs occurs during drawing of the composite film.

On the other hand, the G-peak intensity (VV mode) shows a dependency on the draw ratio of the composite film, as plotted in Figure 7. The plot shows that the orientation of the SWNT increases much amount at the initial stage of drawing followed by decreasing slope with successive drawing.

Electrical Properties of the Composite Films

The change in the electrical conductivity provides information about the overall connectivity of the conducting network and is categorized into three behaviors according to the size and distribution of the conductive clusters [24]. Figure 8 shows the SWNT content dependence of surface resistivity of the composite films with up to 5 wt% of SWNT measured at 25 °C. The composite film exhibits a sudden drop of electrical resistivity at 1 wt% of SWNT loading, as shown in Figure 8, which implies that the threshold loading of SWNT for electrical conductivity is lower than 1wt% for the composite film. This effect is originated from the interwoven fibrous

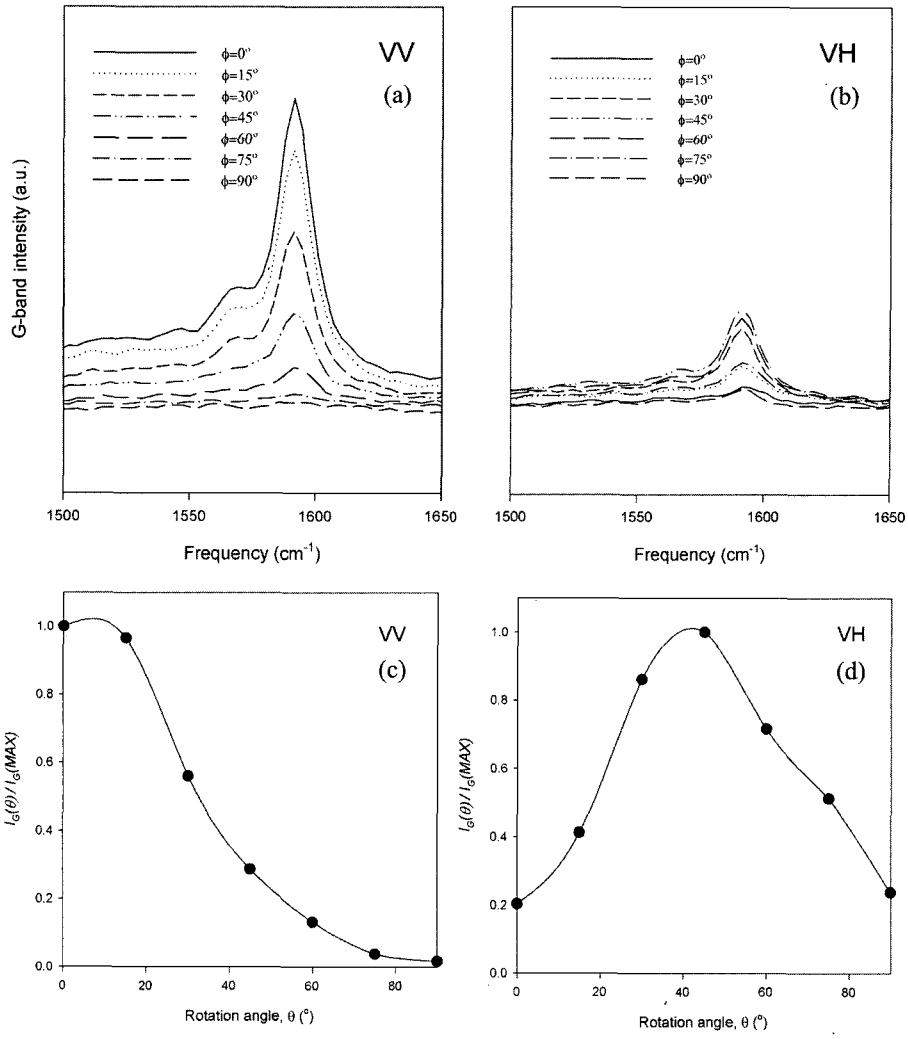

Figure 6. (a) and (b) show the VV and VH G-band Raman spectra taken with different angle (θ) (see text). (c) and (d) show the VV and VH G-band intensity shown in (a) and (b).

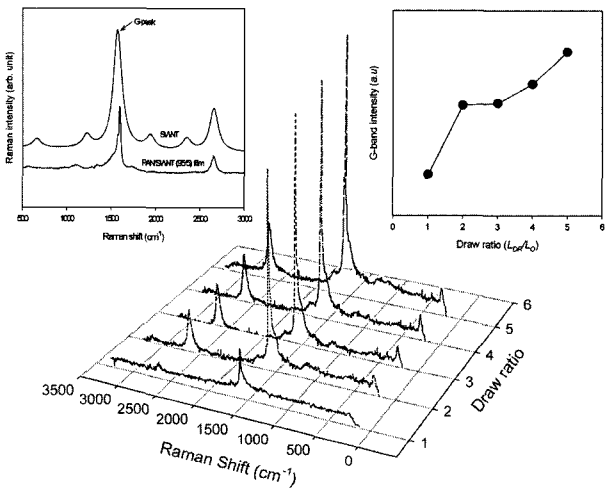

Figure 7. Raman spectra of PAN/SWNT composite film at various draw ratio.

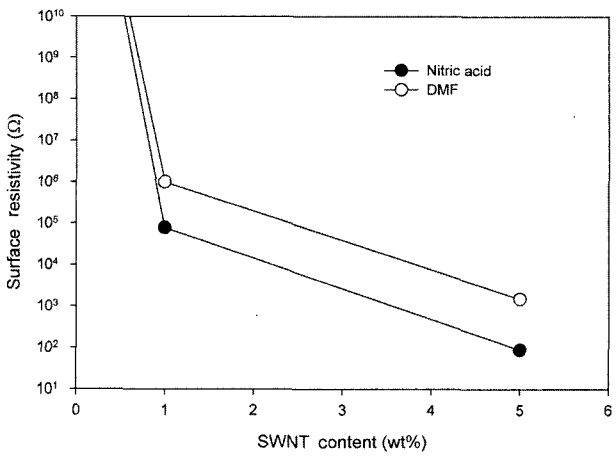

Figure 8. Drop of electrical resistivity of PAN film according to SWNT content and solvent (DMF data from the previous study, ref.[13]).

structure of nanotubes in the composite, which gives rise to conductive passways, as discussed in the AFM image (Figure 4).

The electrical resistivity of the film made using nitric acid was lower than that of the film using DMF when compared to the data in the previous study [13]. Thus, nitric acid is presumably more effective in dispersing nanotubes than DMF.

Conclusions

SWNT was well dispersed in a concentrated nitric acid with help of sonication. The interfacial adhesion between PAN and SWNT was strong enough to break the nanotube at the crack of the composite film. Raman spectra proved good orientation of SWNT along to the drawing axis of the film. From the result of the electrical properties of the composite films, the dispersity of SWNT in nitric acid seems to be better than that in DMF.

Acknowledgements

This research was supported by Kumoh National Institute of Technology.

References

1. B. Schartel, P. Pötschke, U. Knoll, and M. Abdel-Goad, *Euro. Polym. J.*, **41**(5), 1061 (2005).
2. R. H. Baughman, A. A. Zakhidov, and W. A. de Heer, *Science*, **297**, 787 (2002).
3. D. W. Ferguson, E. W. S. Bryant, and H. C. Fowler, *ANTEC'98*, 1219 (1998).
4. B. Lahr and J. Sandler, *Kunststoffe*, **90**, 94 (2000).
5. D. Qian, E. C. Dickey, R. Andrews, and T. Rantell, *Appl. Phys. Lett.*, **76**, 2868 (2000).
6. J. K. W. Sandler, S. Pegel, M. Cadek, F. Gojny, M. van Es, J. Lohmar, W. J. Blau, K. Schulte, A. H. Windle, and M. S. P. Shaffer, *Polymer*, **45**, 2001 (2004).
7. G. Beyer, *Fire Mater.*, **26**, 291 (2002).
8. T. Kashiwagi, E. Grulke, J. Hilding, R. Harris, W. Awad, and J. Douglas, *Macromol. Rapid Commun.*, **23**, 761 (2002).
9. G. Beyer, *Gummi Fasern Kunstst*, **55**, 596 (2002).
10. T. Kashiwagi, E. Grulke, J. Hilding, K. Groth, R. Harris, K. Butler, J. Shields, S. Kharchenko, and J. Douglas, *Polymer*, **45**, 4227 (2004).
11. K. Lau, M. Lu, C. Lam, H. Cheung, F. Sheng, and H. Li, *Comp. Sci. and Tech.*, **65**(5), 719 (2005).
12. T. V. Sreekumar, T. Liu, B. G. Min, H. Guo, S. Kumar, and R. H. Hauge *et al.*, *Adv. Mater.*, **16**, 58 (2004).
13. S. H. Kim, B. G. Min, S. C. Lee, S. B. Park, T. D. Lee, M. Park, and S. Kumar, *Fibers and Polymers*, **5**(3), 198 (2004).
14. A. R. Bhattacharyya, T. V. Sreekumar, T. Liu, S. Kumar, L. M. Ericson, R. H. Hauge, and R. E. Smalley, *Polymer*, **44**, 2373 (2003).
15. T. V. Sreekumar, T. Liu, B. G. Min, H. Guo, S. Kumar, R. H. Hauge, and R. E. Smalley, *Adv. Mater.*, **16**, 58 (2004).
16. J. Liu, M. J. Casavant, M. Cox, D. A. Walters, P. Boul, W. Lu, A. J. Rimberg, K. A. Smith, D. T. Colbert, and R. E. Smalley, *Chem. Phys. Lett.*, **303**, 125 (1999).
17. J. M. Bonard, T. Stora, J. P. Salvetant, F. Maier, T. Stockli, C. Duschl, L. Forro, W. A. de Heer, and A. Chatelain, *Adv. Mater.*, **9**(10), 827 (1997).
18. W. Huang, Y. Lin, S. Taylor, J. Gaillard, A. M. Rao, and Y-P. Sun, *Nano Letters*, **2**(3), 231 (2002).
19. M. S. Dresselhaus and P. C. Eklund, *Adv. Phys.*, **49**, 705 (2000).
20. M. A. Pimenta, A. Marucci, S. A. Empedocles, M. G. Bawendi, E. B. Hanlon, A. M. Rao, P. C. Eklund, R. E. Smalley, G. Dresselhaus, and M. S. Dresselhaus, *Phys. Rev. B*, **58**, R16016 (1998).
21. S. D. M. Brown, A. Jorio, P. Corio, M. S. Dresselhaus, G. Dresselhaus, R. Satio, and K. Kneipp, *Phys. Rev. B*, **63**, 155411 (2001).
22. A. Jorio *et al.*, *Phys. Rev. B*, **65**, 121402 (2002).
23. G. S. Duesberg, I. Loa, M, Burghard, K. Syassen, and S. Roth, *Phys. Rev. Lett.*, **85**(25), 5436 (2000).
24. Y. J. Kim, T. S. Shin, H. D. Choi, J. H. Kwon, Y. C. Chung and H. G. Yoon, *Carbon*, **43**(1), 23 (2005).